analytical chemistry

Article

pubs.acs.org/ac

Evaluation of a Droplet Digital Polymerase Chain Reaction Format for DNA Copy Number Quantification

Leonardo B. Pinheiro,*[,†] Victoria A. Coleman,[†] Christopher M. Hindson,[‡] Jan Herrmann,[†] Benjamin J. Hindson,[‡] Somanath Bhat,[†] and Kerry R. Emslie[†]

[†]National Measurement Institute, Lindfield, New South Wales, Australia

[‡]Bio-Rad Laboratories, Inc., Pleasanton, California, United States

Supporting Information

ABSTRACT: Droplet digital polymerase chain reaction (ddPCR) is a new technology that was recently commercialized to enable the precise quantification of target nucleic acids in a sample. ddPCR measures absolute quantities by counting nucleic acid molecules encapsulated in discrete, volumetrically defined, water-in-oil droplet partitions. This novel ddPCR format offers a simple workflow capable of generating highly stable partitioning of DNA molecules. In this study, we assessed key performance parameters of the ddPCR system. A linear ddPCR response to DNA concentration was obtained from 0.16% through to 99.6% saturation in a 20,000 droplet assay corresponding to more than 4 orders of magnitude of target DNA copy number per ddPCR. Analysis of simplex and duplex assays targeting two distinct loci in the Lambda DNA genome using the ddPCR platform agreed, within their expanded uncertainties, with values obtained using a lower density microfluidic chamber based digital PCR (cdPCR). A relative expanded uncertainty under 5% was achieved for copy number concentration using ddPCR. This level of uncertainty is much lower than values typically observed for quantification of specific DNA target sequences using currently commercially available real-time and digital cdPCR technologies.

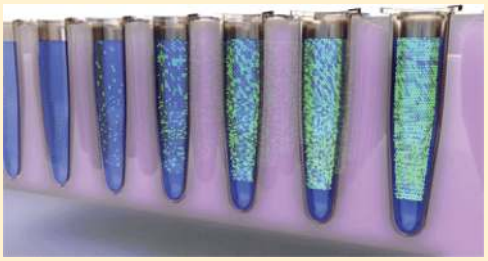

The ability to quantify nucleic acids with accuracy and precision is fundamental to many fields of basic research, molecular diagnostic tests, and commercial processes. Although real-time polymerase chain reaction (PCR) has found widespread utility for nucleic acid quantification, it requires the comparison of an unknown to a standard to obtain quantitative information. Real-time PCR is an analogue measurement based on monitoring amplification after each cycle of PCR using fluorescence probes. The point at which the reaction fluorescence crosses an intensity threshold is called the cycle threshold (Ct). As many factors can influence PCR efficiency and hence the Ct value, the accuracy and precision of real-time PCR can vary widely.

The principle of digital PCR was first introduced in the 1990s[1,2] and is increasingly being utilized for quantification of DNA targets.[3−5] Digital PCR is an end-point measurement that provides the ability to quantify nucleic acids without the use of standard curves. In a typical digital PCR experiment, the sample is randomly distributed into discrete partitions, such that some contain no nucleic acid template and others contain one or more template copies. The partitions are thermally cycled to end-point and then read to determine the fraction of positive partitions, from which the concentration is calculated using eq 1.

$$M = -\ln\left(1 - \left(\frac{P}{R}\right)\right) \text{copy number per droplet} \quad (1)$$

where M is the average number of target molecules per partition, P is the number of partitions containing amplified product, and R is the number of partitions or reactions analyzed.[6]

Two key factors influence the reliability of digital PCR measurements: the number of reactions analyzed (R) and the number of template molecules in the assay.[7] Since concentration is derived by dividing the copy number estimate by the assay volume, an additional key factor, partition volume (V_d) (and its associated uncertainty) needs to be considered when measuring DNA concentration using digital PCR.

Currently, the commercially available microfluidic chamber based digital PCR (cdPCR) formats contain up to a few thousand individual reactions or microfluidic chambers for each technical replicate. Using these formats, confidence in the estimated copy number can be improved by increasing the number of technical replicates and hence, the total number of reactions analyzed. However, there have been practical limitations, primarily cost, to the number of technical replicates that can be analyzed by cdPCR. A new dPCR format called Droplet Digital PCR (ddPCR) has recently been commercialized.[8] A single ddPCR is comprised of approximately 20 000 partitioned droplets, a number which is about 25 times the 765

Received: September 29, 2011
Accepted: November 28, 2011
Published: November 28, 2011

   dx.doi.org/10.1021/ac202578x | Anal. Chem. 2012, 84, 1003−1011

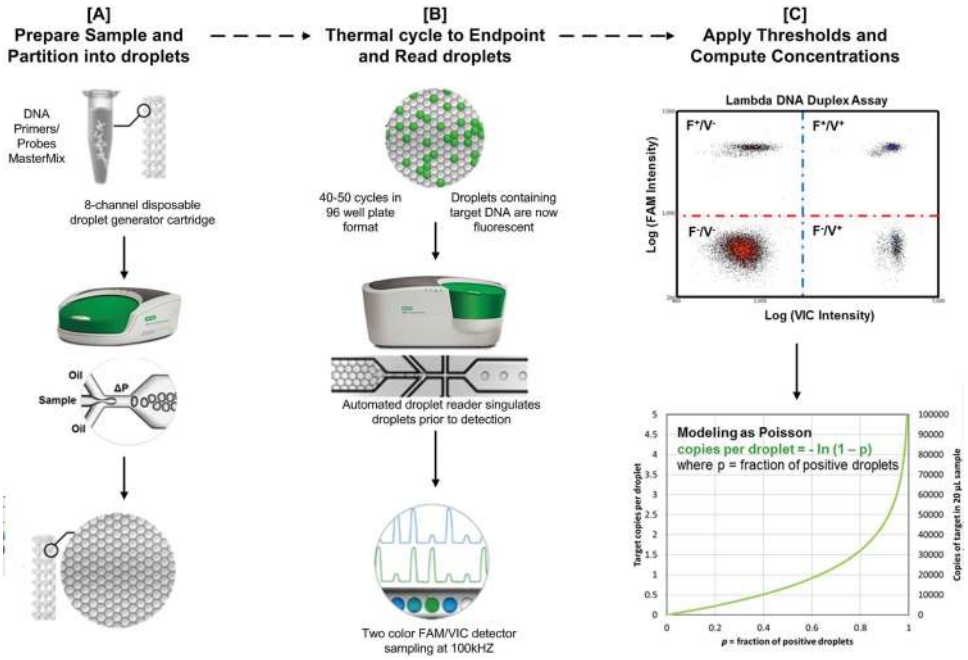

Figure 1. Schematic showing the ddPCR workflow. (A) Each 20 μL sample containing the Master Mix, primers, TaqMan probes, and DNA target is loaded in the middle wells of a disposable eight channel droplet generator cartridge (pictured). Droplet generation oil (8 × 60 μL) containing the emulsion stabilizing surfactant is then loaded into the left-hand wells of the droplet generator cartridge. A vacuum is automatically applied to the outlet well (right) creating a pressure difference that, together with the geometry of the microfluidic circuit, converts the aqueous sample into stable, monodisperse, water-in-oil droplet emulsions which concentrate due to density differences from the oil phase and accumulate in the droplet collection wells of the cartridge. The droplets from each well are then transferred to one well of a 96-well plate, foil sealed, and thermal-cycled to the end-point. (B) After amplification, the plate is then loaded to a droplet reader where an autosampler aspirates the droplets and, using a microfluidic singulator, streams them single file (~1500 droplets/s) past a FAM/VIC two color fluorescence detector which samples at a rate of 100 kHz. (C) The difference in fluorescence amplitudes for droplets where amplification has or has not occurred (positive and negatives, respectively) divides the entire droplet population into four discrete clusters for a typical Fam/Vic duplex assay. These four populations are droplets containing either no target (F−/V−), one of the targets (F−/V+, F+,V−), or both targets (F+,V+). Setting a fluorescence threshold for each detection channel affords a digital method of droplet classification and computing the average number of copies per droplet based on the fraction of positive droplets and Poisson modeling.

chambers of a single sample panel on a microfluidic cdPCR array.

In this study, we evaluated key factors that can influence the reliability of results obtained from an early access beta-prototype ddPCR system (Bio-Rad, Pleasanton, CA). The linearity of the response and the precision over the dynamic range of the 20 000-droplet assay (referred to as 20 000-ddPCR) were assessed. Since the droplets are generated from a single-use eight channel droplet generator cartridge, we examined both the intra- and inter-cartridge repeatability of assays. Copy number concentration and ratio together with their expanded uncertainties were assessed using both a high density ddPCR technology and a lower density cdPCR platform.

EXPERIMENTAL SECTION

Lambda DNA Solution and PCR Assays. Lambda DNA solution (Fermentas) was analyzed using the primer and probe sequences and concentrations for assays 2 and 5 as previously described.[9] (Table S-1 in the Supporting Information). Assays 2 and 5 target different regions of the Lambda DNA genome (5′ base of the amplicon is 16 541 and 44 925, respectively, in the 48 502 base pair Lambda DNA genome) and produce amplicons of 188 and 76 base pair (bp), respectively.[9] The Lambda DNA was used as supplied and not physically or enzymatically treated to reduce fragment length prior to analysis.

Droplet Digital PCR Instrumentation, Workflow, and Data Analysis. All experimental work including ddPCR and droplet volume measurements was conducted at the National Measurement Institute, Australia. Reaction mixtures of 20 μL volume comprising 1× ddPCR Master Mix (Bio-Rad), relevant forward and reverse primers and probe(s) (Table S-1 in the Supporting Information), and DNA were prepared using a gravimetric protocol to minimize the uncertainty due to pipetting. The ddPCR reagents, except DNA, were premixed and the final reaction mix was prepared gravimetrically by combining the DNA and PCR components (Supporting Information S-1). Each 20 μL reaction was dispensed into a separate well of a disposable eight channel droplet generator cartridge (Figure 1A; Bio-Rad). A volume of 60 μL of droplet generation oil (Bio-Rad) was then loaded into each of the corresponding oil wells before the consumable chip was loaded into a beta-prototype droplet generator (Bio-Rad). The droplet generator applies a vacuum to each of the outlet wells to generate droplets in the eight channels simultaneously at a rate of ~1 000 droplets/channel/second until the complete 20 μL ddPCR mixture has been partitioned into the monodisperse water-in-oil emulsion format. Each water-in-oil emulsion was transferred by pipet to a separate well of a 96-well polypropylene plate (Eppendorf), heat sealed with foil, and amplified in a conventional calibrated thermal cycler (Eppendorf Mastercycler ep "S" thermocycler). Thermal cycling conditions consisted of a 10 min activation period at

dx.doi.org/10.1021/ac202578x | Anal. Chem. 2012, 84, 1003−1011

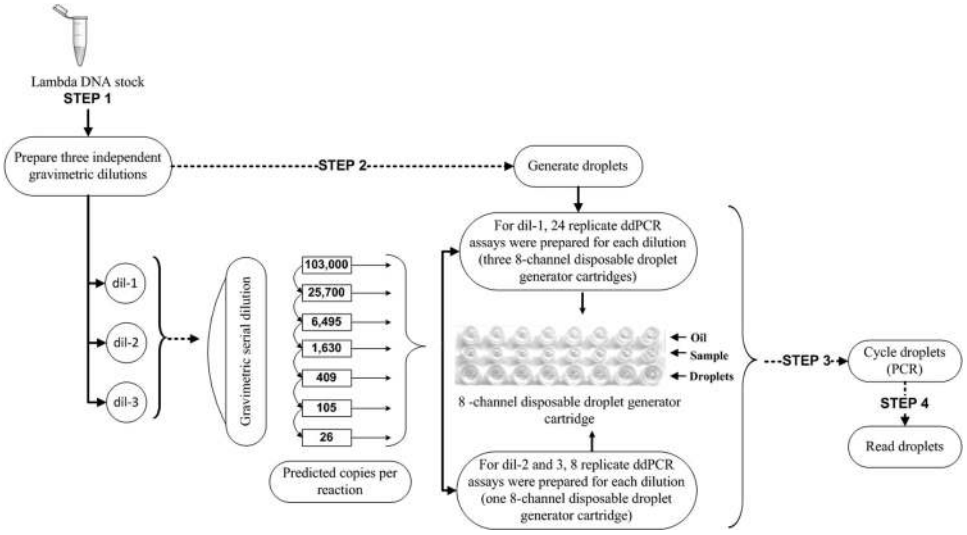

Figure 2. Schematic diagram of experimental design for assessing linearity and precision.

95 °C followed by 40 cycles of a two step thermal profile of 15 s at 94 °C denaturation and 60 s at 60 °C for combined annealing-extension at 100% ramp rate and a final 10 min inactivation step at 98 °C. After thermal cycling, plates were transferred to a beta-prototype droplet reader (Bio-Rad) that employs an integrated autosampler and fluidics to serially aspirate droplets from each well and stream them single-file, at a rate of ~1 500 droplets/second, past a two-color fluorescence detector sampled at a rate of 100 kHz on both FAM and VIC fluorescence channels (Figure 1B). Sampling at 100 kHz affords the ability to gate outliers on a case-by-case basis using properties of the fluorescence trace (automated by Bio-Rad Signal Processing Algorithm v0.43). Discrimination between droplets that did not contain target (negatives) and those which did (positives) was achieved by applying a global fluorescence amplitude threshold in QuantaSoft (Bio-Rad), the software package provided with the ddPCR system for data acquisition and analysis. The droplet reader was calibrated once upon installation of the ddPCR system at the National Measurement Institute, Australia. The simple calibration procedure generated an instrument-specific color compensation matrix that was subsequently stored on the droplet reader and automatically applied to data to eliminate cross talk between FAM and VIC labeled probes. The QuantaSoft software had a factory preset value for droplet volume. QuantaSoft uses a proprietary signal-processing algorithm to automatically perform droplet gating within each run. The threshold was set as the midpoint between the average fluorescence amplitude of positives and negative droplet clusters on each of the FAM and VIC channels (Figure 1C). Droplets appeared stable through the entire process including pipet manipulations, thermal cycling, and reading. Rejection criteria for excluding a well from subsequent analysis during our dynamic range studies on the prototype droplet reader included (i) a clog detected by the Bio-Rad Signal Processing Algorithm software of the droplet reader or (ii) a low number of droplets measured per 20 μL PCR.

Digital PCR Instrumentation and Data Analysis. Digital PCR analysis was performed using 12.765 digital arrays on a BioMark System (Fluidigm, South San Francisco) (referred to as 765-cdPCR). The final reaction mix for each digital panel comprised 1000 predicted copies of Lambda DNA, 1× ABI Taqman FAST PCR Mastermix with no UNG AmpErase (Applied Biosystems Melbourne, Australia), 1× sample loading reagent (Fluidigm, South San Francisco), and relevant forward and reverse primers and probe (Table S-1 in the Supporting Information). To minimize the uncertainty from pipetting, all PCR components excluding DNA were premixed and then the final reaction mix was prepared gravimetrically by combining the DNA and PCR components. A volume of 10 μL of the reaction mix was aliquoted into each sample inlet on the digital array with approximately 4.6 μL of the reaction mix distributed throughout the partitions within each panel using an automated MX Integrated Fluidic Circuit (IFC) Controller (Fluidigm, South San Francisco). The chip setup was randomized. No Template Controls (NTC) containing 1× $TE_{0.1}$ buffer (10 mM Tris, 0.1 mM EDTA, pH 8.0) in place of DNA or blank panels containing 1× $TE_{0.1}$ buffer in place of DNA and primer/probes were analyzed in one or more alternate panels. Blank panels were used in order to accommodate the chip-setup (Figure S-1 in the Supporting Information). Digital array thermal cycling conditions consisted of a 2 min activation period at 95 °C, followed by 50 cycles of a two-step thermal profile involving 10 s at 95 °C for denaturation, and 30 s at 60 °C, for combined annealing and extension. The data was analyzed using BioMark data analysis software (v3.0.2) using a manually set quality threshold of 0.01 and target Ct range of 15−50.

Linearity and Precision over Theoretical Dynamic Range of ddPCR Instrument. Three independent gravimetric serial dilutions of Lambda DNA were prepared using a standard protocol (Supporting Information S-1) to produce three sets of seven solutions containing an average 26, 105, 409, 1 630, 6 495, 25 700, and 103 000 predicted copies of Lambda DNA per 20 μL ddPCR based on absorbance measurements of the stock Lambda DNA solution at 260 nm (Figure 2). For two of the serial dilution sets (gravimetric dilution series 2 and 3), eight replicate ddPCRs were prepared from a single eight-channel droplet generator cartridge for each of the seven solutions. For gravimetric dilution series 1, 24 replicate ddPCRs were prepared from three eight-channel droplet generator cartridges for each of the seven solutions. The ddPCRs were analyzed using assay 2 under simplex conditions. A complete eight channel cartridge of NTC was prepared by adding 1× $TE_{0.1}$ buffer in place of DNA template. NTCs showed a

dx.doi.org/10.1021/ac202578x | *Anal. Chem.* 2012, 84, 1003−1011

low-level background signal of approximately three positive droplets per NTC assay, which could possibly be attributed to low-level template contamination during the preparation of the reaction mixture. The data generated was used to assess linearity and precision over the theoretical dynamic range of the instrument in addition to intracartridge and intercartridge ddPCR precision.

Comparison of DNA Concentration and Ratio Measurements Using Two Different dPCR Formats under Simplex and Duplex Conditions. Three independent gravimetric serial dilutions of Lambda DNA were prepared. For each gravimetric dilution series, one dilution was selected for analysis using both 20 000-ddPCR and 765-cdPCR. This dilution provided a predicted number of 1.3 copies per 6 nL reaction (based on A_{260} measurement of NaOH denatured stock Lambda DNA[9]) for the microfluidic 765-cdPCR which is close to the optimal 1.5 molecules per reaction for minimizing the uncertainty of the copy number estimate.[10] Since the droplet volume is approximately one-sixth of the chamber volume, the predicted number of copies per 1 nL droplet volume was 0.2 copies per droplet which is less than the optimal number for this digital PCR format. For each of the three gravimetric dilutions, five replicate ddPCR and five replicate microfluidic cdPCR were prepared and analyzed. The ddPCRs droplets were generated from one eight channel droplet generator cartridge, and the replicates were transferred to separate wells within a single column of a 96-well plate for thermal cycling and droplet reading. A total of 15 NTCs containing 1× $TE_{0.1}$ in place of DNA template were similarly prepared and transferred to three individual columns (five replicas assays each) of the 96-well plate. NTCs showed a low-level background signal of approximately two positive droplets per NTC assay. The microfluidic cdPCR assays were prepared and then analyzed across two 12.765 chips (randomly designated to two panels in one chip and three panels in the other chip). Each microfluidic cdPCR experiment contained either one or two NTC panels per chip. All NTC panels were negative. For ddPCR and microfluidic cdPCR, the replicate assays were analyzed using assay 2 under simplex conditions. A similar experimental setup was used for analysis with assay 5 under simplex conditions and for both assays 2 and 5 under duplex conditions.

Optical Microscope Imaging to Determine Droplet Volume. The average droplet volume was independently measured at the National Measurement Institute, Australia, to compare with that quoted by the ddPCR instrument manufacturer (BioRad, personal communication), by measurement of droplets generated from 16 different channels. Droplets used for optical imaging to determine droplet volume were prepared using the same reagents as used for ddPCR estimation of Lambda DNA concentration. Either three or four wells were randomly selected from each of five different droplet generator cartridges for this analysis. Between 61 and 77 droplets were measured from each channel providing measurement of 1 122 droplets in total.

The droplets were transferred by pipet into 1 μ-Slide VI flat uncoated microscopy chambers (IBIDI Germany) that had been prefilled with droplet generation oil (Bio-Rad). After filling, the slides were gently held at an angle to allow a uniform monolayer of droplets to develop at the upper oil−slide interface for imaging. An optical microscope (Leica DM6000M) with a digital CCD camera (Leica DFC490) was used to image the droplets. Images were recorded under uniform illumination in a bright field, using a HC PL FLUOTAR 20×/0.50 BD/Coverglass: O/ICT upright: K2+D (K3+D1)/ICR: D1/D/thread: M32/FWD: 1.27 objective with numerical aperture 5, to produce images at 200× apparent magnification. A 12 V 100 W tungsten halogen lamp was used as the illumination source. Digital images were collected on a computer running the Leica Application Suite Software v3.5. Images were captured in interlaced large high-quality format, corresponding to an image size of 3264 × 2448 pixels.

The x and y length scales of the microscope/camera system were calibrated using a stage micrometer, model MW-1540. Calibration values indicated the CCD comprised a square pixel array to within the limits of relative uncertainty of the scale bar measurement of 0.1%. The calibration was repeated by placing one 1 μ-Slide VI filled with droplet generation oil over the micrometer features to investigate the impact of refractive index differences of the slide−oil interface. A change of the calibration of less than 0.1% was observed which is of the same order as the uncertainty of the calibration.

ImageJ software v1.42[11] was used for analysis of the digital images. Images were first converted to a bit depth of 8-bit for processing. The edges of the droplets were identified using the "find edges" algorithm. The image was then inverted, and the edges of the droplets were identified by thresholding the images. To enable detection of the full droplet, a "fill holes" algorithm was run after noise reduction and despeckling. The image was then thresholded again to achieve detection of the entire droplet. The watershed algorithm implemented in the ImageJ software was used to separate touching droplets. Droplets on the edge of the image were excluded from analysis.

The binary images of the droplets were then analyzed. The major and minor axis of an elliptical fit to the droplet outline were determined and used to calculate the area in $(\text{pixels})^2$ of an ellipse of equivalent dimensions. This value was then used to determine the diameter of a circle of an equivalent area. This equivalent circular diameter, measured in pixels, was converted to length units by applying the conversion factor between the length measured in pixel units and length measured in micrometers determined from the instrument calibration. Finally, the equivalent spherical volume of a sphere having the equivalent circular diameter was calculated.

The sensitivity of the droplet size to the focus was investigated by analyzing images taken at focal planes displaced by up to ±6 μm from ideal focus. The resulting variation of the measured volume due to minor out of focus variation introduced during image data collection was found to be less than 1.4% (Figure S-2 in the Supporting Information).

Determination of Stock DNA Copy Number Concentration from ddPCR and cdPCR Data. The number of accepted droplet reactions in each ddPCR, R, was between 10 000 and 18 000. The droplet copy number concentration, T_d, was calculated by multiplying M by $1000/V_d$, where V_d is the mean droplet volume (nL) (eq 2).

$$T_d = \frac{-1000}{V_d} \ln\left(1 - \left(\frac{P}{R}\right)\right) \text{ copy number per } \mu\text{L} \quad (2)$$

The template DNA concentration in the original stock solution, T, can then be calculated by multiplying T_d by the total dilution factor, D, used to dilute the stock DNA solution into the final ddPCR solution (eq 3).

dx.doi.org/10.1021/ac202578x | Anal. Chem. 2012, 84, 1003−1011

$$T = \frac{-D \times 1000}{V_d} \ln\left(1 - \left(\frac{P}{R}\right)\right)$$

copy number per μL stock solution (3)

To estimate the template copy number concentration using a 12.765 cdPCR chip, R was substituted with 765 in the above equations since this is the number of chambers per panel.

Estimation of Measurement Uncertainty. Measurement uncertainty was estimated using a top-down approach. Experimental data from independent sets (such as independent gravimetric dilutions) and replicate measurements was combined using the pooled relative standard deviation. Equations 4 and 5 were used for precision data for M and copy number ratio, respectively, where n_i is the number of replicates in the ith data set and CNR_i is the ratio of the copy number concentration determined between assays 5 and 2. Equation 4 captures the precision of the copy number estimate from Poisson modeling as well as other Type A components such as any variation in the volume of droplets generated from different channels of the droplet generator or in the preparation of the gravimetric dilution series.

$$\frac{SD_{M_{prec}}}{\bar{M}} = \sqrt{\frac{\left(\frac{SD_{M_1}}{M_1}\right)^2\left(n_1 - 1\right) + \left(\frac{SD_{M_2}}{M_2}\right)^2\left(n_2 - 1\right)... + \left(\frac{SD_{M_i}}{M_i}\right)^2\left(n_i - 1\right)}{n_1 + n_2... + n_i - i}} \quad (4)$$

$$\frac{SD_{CNR}}{\overline{CNR}} = \sqrt{\frac{\left(\frac{SD_{CNR_1}}{CNR_1}\right)^2\left(n_1 - 1\right) + \left(\frac{SD_{CNR_2}}{CNR_2}\right)^2\left(n_2 - 1\right)... + \left(\frac{SD_{CNR_i}}{CNR_i}\right)^2\left(n_i - 1\right)}{n_1 + n_2... + n_i - i}} \quad (5)$$

The relative standard uncertainty of the precision data was then determined by dividing the pooled relative standard deviation by the square root of the number of data sets as shown in eqs 6 and 7, respectively.

$$\frac{u_{M_{prec}}}{\bar{M}} = \frac{SD_{M_{prec}}}{\bar{M}\sqrt{i}} \quad (6)$$

$$\frac{u_{CNR_{prec}}}{\overline{CNR}} = \frac{SD_{CNR}}{\overline{CNR}\sqrt{i}} \quad (7)$$

The relative standard uncertainty of the droplet volume, $(u_{V_d})/(\bar{V}_d)$, is a Type B uncertainty evaluation (obtained from information such as calibration certificates and limits deduced from personal experience[12]) and was determined from the analysis of an individual droplet image. Factors such as the goodness of the elliptical fit, operator bias, microscope calibration, and effect of focus were all considered in the estimation of this uncertainty. The combined standard uncertainty of the concentration based on the top-down approach, $u(T)$, was calculated by combining the precision data (Type A uncertainty component evaluated by statistical analysis of a series of measurements) with a Type B uncertainty component associated with measurement of the droplet volume using eq 8. A full assessment of bias using this prototype instrument was not feasible. However, the dynamic range experiment and the comparison with an independent cdPCR system provided data to make an assessment of bias from the measurements of M.

$$u(T) = T\sqrt{\left(\frac{u_{V_d}}{\bar{V}_d}\right)^2 + \left(\frac{u_{M_{prec}}}{\bar{M}}\right)^2}$$

copy number per μL stock solution (8)

The standard uncertainty of the copy number ratio based on the top-down approach, u_{CNR}, was equivalent to the standard uncertainty of the precision data, $u_{CNR_{prec}}$. Since the assays were run under duplex conditions, the uncertainty associated with droplet volume is minimized and was not considered in this estimation.

The expanded uncertainty was calculated by multiplying the standard uncertainty by a coverage factor[12] which provides a level of confidence of 95% that the true value for the measurand falls within the expanded uncertainty. The coverage factor varied from 2.05 to 2.18 depending on the effective degrees of freedom which was derived from the Welch-Satterthwaite formula[12] and was influenced by the number of replicates and independent data sets analyzed in each experiment.

RESULTS AND DISCUSSION

Dynamic Range. The theoretical dynamic range in digital PCR is largely determined by the number of partitions that are analyzed. A typical ddPCR contains approximately 20 000 individually partitioned droplet reactions. On the basis of binomial approximation, 99.5% saturation of the droplets (i.e., 100 negative droplets in a ddPCR containing 20 000 droplets) would indicate between 102 000 and 110 000 copies of target DNA (95% confidence interval) in the 20 000-droplet reaction. This provides a theoretical dynamic range of 10^5 target copies.

We examined the ddPCR response over concentrations ranging from approximately 37 to 131 000 copies per 20 μL of ddPCR. This resulted in as little as 0.16% positive droplets through to almost complete saturation (99.6% positive droplets). The study, which included data from three independent gravimetric dilution series, comprised a total of 168 ddPCRs. Less than 5% of these assays were excluded from data analysis. Five assays were excluded because a clog was detected by the droplet reader software and an additional three assays were excluded because either no droplets or only 192 droplets were detected by the droplet reader. The average number of droplets read for each ddPCR was 13,825 with a standard deviation of 1,892 droplets.

The ddPCR response was linear over this dynamic range, which covered more than 4 orders of magnitude (r^2 = 0.9994; Figure 3a). However, as previously described for cdPCR,[7] the relative uncertainty in concentration was not constant across the dynamic range. The stochastic effect associated with sampling a DNA solution increases as the concentration of the DNA solution decreases. Consequently, as the copy number concentration of a sample decreases, the number of target DNA molecules in replicate ddPCR assays is more variable. This is reflected in the relative expanded uncertainty of the estimated stock DNA concentration which was 30 and 13% for the assays containing 37 and 142 copies, respectively, per 20 μL of ddPCR. In comparison, the relative expanded

dx.doi.org/10.1021/ac202578x | Anal. Chem. 2012, 84, 1003−1011

uncertainty for assays containing between 2 200 and 33 000 copies was between 4.6 and 6.0% (Figure 3b). When analyzing low template copies, the relative expanded uncertainty of the ddPCR system was slightly lower than the values of 30−56% and 40−60% reported recently for a 765-cdPCR assay containing either 16 or 128 copies, respectively.[3]

The Lambda DNA stock concentration was estimated from seven gravimetrically prepared dilutions of the stock solution that covered the above range and all results agreed within their expanded uncertainties. The highest concentration analyzed (131 000 copies per ddPCR) contained, on average, 6.5 copies per droplet which is 30% greater than the manufacturer's recommended upper concentration limit of five copies per droplet, on average (Bio-Rad, personal communication). For this highly concentrated ddPCR data set, 99.6% of droplets were positive. While the stock concentration estimation from this data set was slightly lower than the average, it still agreed within its expanded uncertainty with the other data sets (Figure 3b). Using ANOVA analysis, there was no significant difference ($p > 0.05$) in the estimated concentration of the Lambda stock when the 20 μL of ddPCR contained between 463 and 28 900 copies (p = 0.685, 0.243, and 0.463 for the three independent gravimetric dilutions).

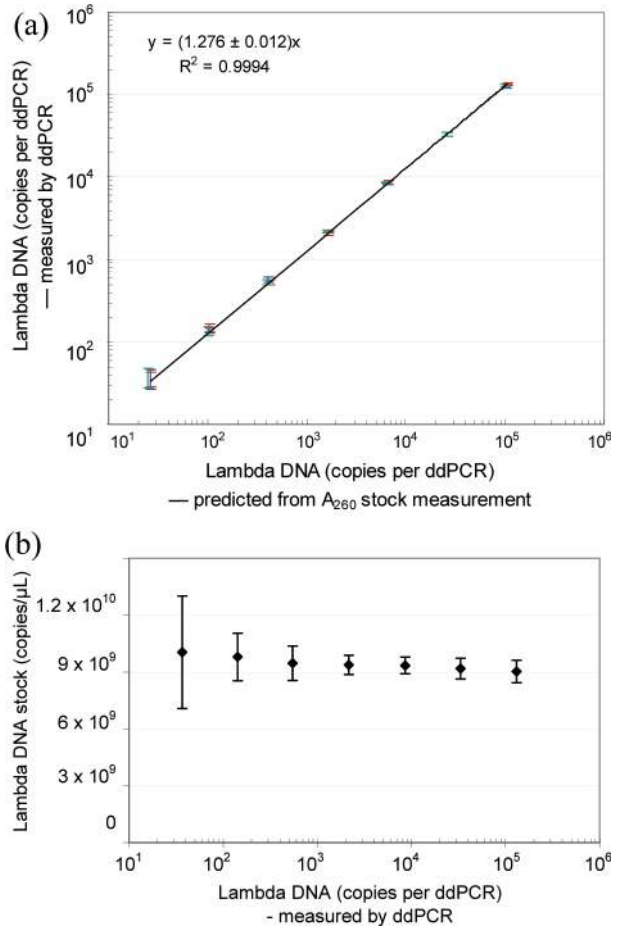

Figure 3. (a) Linearity and (b) precision across the dynamic range of ddPCR. (a) Red, green, and blue error bars denote the standard deviation of the Lambda DNA copy number per 20 μL of ddPCR for each of three independent gravimetric dilutions (estimated from n = 7 or 8 replicates in each case). The 95% confidence interval of the slope of the combined data is as indicated in the equation. (b) Each symbol denotes the stock Lambda DNA concentration (copies/μL) (estimated from n = 7 or 8 replicates for each of three independent gravimetric dilutions). Error bars represent the expanded uncertainty calculated by multiplying the combined standard uncertainty (eq 8) with a coverage factor of between 2.05 and 2.09 depending on the number of replicates in the independent gravimetric dilutions. This provides a level of confidence of 95% in the expanded uncertainty.

Accuracy of ddPCR by Comparison with Independent cdPCR Measurement System. Typically, accuracy of a measurement is assessed by the closeness of agreement between the measured value and a true quantity value or an accepted reference value of a measurand.[12] In the absence of a DNA reference material certified for absolute copy number concentration, results obtained from the ddPCR system were compared with results obtained from a 765-cdPCR platform. Both systems provide a measurement of the absolute copy number concentration without the need for an external calibrant.

Lambda DNA concentrations (copies/μL) and ratios measured using the 20 000-ddPCR and 765-cdPCR formats were compared using two assays that target different regions of the Lambda genome (assays 2 and 5) (Table 1).[7] Regardless of the assay used, the Lambda DNA concentration measurements using the 20 000-ddPCR and the 765-cdPCR agreed within their expanded uncertainties, which were estimated by multiplying the combined standard uncertainty (eq 8) with a coverage factor between 2.05 and 2.13 to provide a level of confidence of 95%. The relative expanded uncertainties for the 20 000-ddPCR were 3.2% and 4.2% for assay 5 and assay 2, respectively, while for the 765-cdPCR the relative expanded uncertainties were 13% and 15%, respectively. The combination of a lower uncertainty in partition volume together with an increase in the number of partitions analyzed has resulted in a lower uncertainty for copy number concentration using ddPCR compared to the microfluidic cdPCR even though the concentration analyzed was most suited to minimizing precision for the chamber microfluidic cdPCR format (see Experimental Section, Comparison of DNA Concentration and Ratio Measurements Using Two Different dPCR Formats under Simplex and Duplex Conditions). For ddPCR using assay 2, measurement precision contributed 77% of the combined total uncertainty (Figure 4b). Approximately 9% of the Type A precision component of the total uncertainty could be attributed to the copy number per droplet measurement, M, which is determined using Poisson modeling, and 3% was attributed to the gravimetric dilution steps. The remainder could be mainly attributed to the variation in volume of droplets generated from different wells of the droplet generator cartridge (Figure S-3 in the Supporting Information). The major component of the Type B droplet volume uncertainty was the estimation of the out-of-plane ellipsoid axis. The much larger uncertainty for the 765-cdPCR was predominantly due to the uncertainty associated with measurement of the z-axis of the chamber volume using optical microscopy, as previously described,[7] and this would also be the case if multiple panels on the higher density microfluidic 48.770 chip (Fluidigm) were analyzed to achieve a similar number of total reactions as for the 20 000-ddPCR. If the z-axis could be measured using a technique with lower uncertainty, this may reduce the uncertainty of the chamber volume and the overall uncertainty of cdPCR measurements using a chamber format. However, 18 panels on the 48.770 chip would be required to obtain 13 860 partitions,

dx.doi.org/10.1021/ac202578x | Anal. Chem. 2012, 84, 1003−1011

Table 1. Comparison of Copy Number Concentration, T, and Ratio Measurements Using Two Digital PCR Formats[a]

simplex				
assay	assay 5		assay 2	
digital PCR format	20 000-ddPCR	765-cdPCR	20 000-ddPCR	765-cdPCR
measured Lambda DNA stock concentration, T, (copies/μL) (eq 3)	1.026×10^{10}	1.02×10^{10}	1.085×10^{10}	9.8×10^{9}
relative standard uncertainty of all precision factors, $(u_{M_{prec}}/\bar{M})$ (%) (eq 6)	1.2	4.3	1.7	5.7
relative standard uncertainty (type B components only) of a single droplet/chamber volume, $(uV_d)/\bar{V}_d$ (%)	1.0	4.7	1.0	4.7
expanded uncertainty of $U(T)$, (copies/μL)	0.033×10^{10}	0.13×10^{10}	0.045×10^{10}	1.5×10^{9}
relative expanded uncertainty of $U(T)$, (%)	3.2	13	4.2	15

duplex		
assay	assay 5/assay 2	
digital PCR format	20 000-ddPCR	765-cdPCR
copy number ratio for assay 5/assay 2 (copy/copy)	1.051	1.052
expanded uncertainty of copy number ratio (copy/copy)	0.030	0.064
relative expanded uncertainty of copy number ratio (% U)	2.8	6.1

[a]For the ddPCR assays, the droplet reader counted an average 13 504 gated droplets per well (range from 12 127 to 14 909 droplets per well), while the cdPCR assays contained 765 microfluidic chambers per panel. Each value is derived from five replicate analyses for each of three independent gravimetric dilutions. Replicates contained approximately 4 000 Lambda DNA copies per 20 μL of ddPCR and approximately 1 000 Lambda DNA copies per 4.65 μL of cdPCR. The Lambda DNA stock concentration was determined under simplex conditions using both assay 5 and assay 2. The copy number ratio between assay 5 and assay 2 was determined under duplex conditions. All precision components were captured in one factor. The only known Type B component which was significant enough to require input was from the droplet volume measurement. The expanded uncertainties for the concentration and ratio were determined by multiplying the combined standard uncertainty (eq 8) and the standard uncertainty,$u_{CNV_{prec}}$, respectively, by a coverage factor between 2.05 and 2.18, which provides a level of confidence of 95%. It should be noted the magnitude of the expanded uncertainty values for T vary with concentration.

and this is not a practical approach for most ddPCR applications.

When the number of reactions in digital PCR is less than one thousand, the estimated copy number will tend to be a larger contributor to the uncertainty than the partition volume (Figure 4a). As the number of reactions increases, the confidence associated with the predicted copy number and the copy number concentration improves dramatically. However, at some point, the reaction volume will become a larger contributor to the uncertainty than the copy number measurement. When this point is reached, any additional increase in the number of reactions will only have a small impact on reducing the total uncertainty (Figure 4a). When the number of reactions is more than 10 000, as is the case for ddPCR, copy number measurement can be achieved with a very high level of precision providing there are no other sources of variability (Figure 4a). To translate this potential improvement in precision to the concentration estimate, droplets must be generated consistently from one assay to the next. The ddPCR droplets are generated using an eight channel injection molded cartridge. Significant variation in the size of droplets generated from different wells either within or between cartridges would be reflected in the variation in concentration estimates following ddPCR.

To investigate the intra- and intercartridge copy number concentration repeatability, a ddPCR was prepared from each well in three eight channel cartridges providing a total of 24 replicate ddPCR assays. This process was undertaken for each of the seven dilutions of the Lambda DNA which contained an average 26, 105, 409, 1 630, 6 495, 25 700, and 103 000 predicted copies of Lambda DNA per 20 μL of ddPCR, based on absorbance measurements of the stock Lambda DNA solution at 260 nm. The eight replicate ddPCR from one cartridge were dispensed into the wells of one column of a 96-well plate prior to end-point PCR. For each Lambda DNA dilution, the assays prepared from three replicate cartridges were analyzed in adjacent columns on the same 96-well plate to minimize possible contributions caused by intraplate variability. ANOVA within and between the ddPCR derived from three replicate cartridges demonstrated no significant intracartridge effect at any of the Lambda DNA concentrations analyzed (p-values ranging from 0.124 to 0.716). There was no significant intercartridge effect for seven of the nine dilutions analyzed (p-values ranging from 0.153 to 0.698), implying that any intracartridge variability in the size of droplets generated was similar to that of the intercartridge variability.

To verify the reproducibility of droplet volume, a sample of 1 122 droplets generated from a total of 16 wells located across 5 separate cartridges were imaged, and each droplet volume was measured using image processing (Figure S-3 in the Supporting Information). The mean droplet volume obtained from image processing measurements was 0.868 nL. A Type B uncertainty evaluation of an individual droplet volume measurement estimated the relative expanded uncertainty of this measurement as 2.0% using a coverage factor of 2.04. This measured droplet volume and associated uncertainty agrees with the manufacturer's independently estimated value of 0.89 nL for droplets generated from the eight channel droplet generator cartridges (Bio-Rad, personal communication). The relative standard deviation of the mean interwell droplet volume for the 16 wells was 2.8%. ANOVA demonstrated no significant intracartridge (p = 0.801) or intercartridge (p = 0.053) effect on the partition volume confirming that the observed variation in droplet volume between wells was independent of the cartridge. Provided sufficient numbers of replicate wells are analyzed, this well-to-well variation in droplet volume is likely to be captured within the precision data of replicate concentration measurements (Figure 4b) and was, therefore, not considered as a separate component in the top down uncertainty estimation.

Assuming that the Lambda DNA genome is intact, the copy number ratio between assay 5 and assay 2 should result in a ratio of 1.0. The Lambda DNA copy number ratio between

dx.doi.org/10.1021/ac202578x | Anal. Chem. 2012, 84, 1003−1011

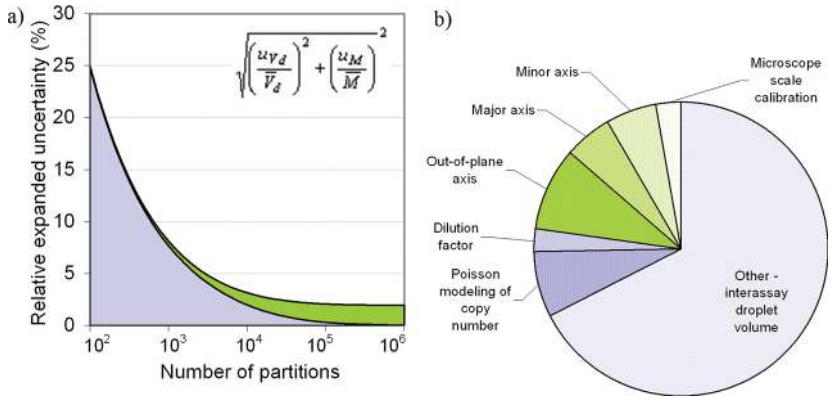

Figure 4. Factors contributing to measurement uncertainty. (a) Theoretical relative expanded uncertainty of concentration considering only two factors: Type B partition volume component, V_d with a relative uncertainty of 1.0% (green), and uncertainty of the Poisson modeling of copy number per droplet, M,[7] (mesh blue) calculated for the condition when 80% of the reactions are positive following digital PCR. This is close to the optimal percentage of positive reactions for minimizing the uncertainty of the copy number estimate, regardless of the number of reactions in the assay.[10] The relative standard uncertainties of these two factors were combined (inset) and then multiplied by two to obtain the relative expanded uncertainty with a level of confidence of 95%. (b) Contributions to concentration uncertainty for a ddPCR data set comprising five replicate analyses from each of three independent gravimetric dilutions analyzed using assay 2 under simplex conditions (see Table 1 for details). This data set had a relative expanded uncertainty of only 4.2%, which was determined by multiplying the combined standard uncertainty (eq 8) by a coverage factor of 2.09 to provide a level of confidence of 95%. The contributions of the components of droplet volume (Type B components only) are indicated in green shading and the components of precision are indicated in blue shading. In this data set, a total of 190 433 droplets were accepted by the droplet reader and 19.1% of these droplets were positive.

assays 5 and 2 under duplex conditions using the 20 000-ddPCR and the 765-cdPCR were 1.051 and 1.052, respectively, and the corresponding relative expanded uncertainties using a coverage factor of 2.18 were 2.8% and 6.1%, respectively (Table 1). The lower expanded uncertainty in copy number variation observed using the 20 000-ddPCR can largely be explained by the more than 20-fold increase in number of partitions analyzed in each ddPCR assay.

CONCLUSIONS

In this study we have demonstrated experimentally that this ddPCR system can achieve a linear dynamic range of more than 4 orders of magnitude for DNA quantification. The large number of reactions in this ddPCR system allowed very precise copy number estimates which resulted in a relative expanded uncertainty of less than 5% for Lambda DNA copy number concentration. Further improvements in uncertainty of absolute copy number quantification may be achieved by increasing the number of replicates analyzed. However, this will be limited by the partition volume uncertainty when it becomes a larger contributor to the uncertainty than the precision of copy number estimates (Figure 4). For duplex copy number ratio measurements, the contribution from partition volume in the uncertainty estimate is minimized since both assays are conducted in the same ddPCR. Therefore, increasing the number of partitions will lead to further improvements in precision, and this can be readily and practically achieved by combining the results of replicate wells.

Because of the high level of precision that can be obtained from ddPCR and other high density cdPCR formats,[13,14] it is particularly important that the experimental design replicates capture all known sources of variation, and that components of bias are identified and included in the uncertainty budget to ensure the measurements are also accurate.[15] For the prototype instrument used in this study, it was difficult to make a full assessment of bias. However, dynamic range studies did not indicate a concentration-dependent bias, and concentration measurements were comparable with results obtained using an independent microfluidic cdPCR. This ddPCR technology should be fit-for-purpose for a wide range of applications, including the direct quantification of nucleic acids for gene expression (e.g., miRNAs), pathogen quantification, rare allele detection, germline and somatic copy number variation estimation, some of which have recently been demonstrated.[8]

ASSOCIATED CONTENT

Supporting Information

Additional information as noted in text. This material is available free of charge via the Internet at http://pubs.acs.org.

AUTHOR INFORMATION

Corresponding Author

*E-mail: Leonardo.Pinheiro@measurement.gov.au. Phone: +61 2 84673735.

ACKNOWLEDGMENTS

The project described was supported by Grant Number R01EB010106 from the National Institute of Biomedical Imaging And Bioengineering (C.M.H., B.J.H.), and the National Enabling Technology Strategy (L.B.P., V.A.C., J.H., S.B., K.R.E.) provided by the Commonwealth Government of Australia. The content is solely the responsibility of the authors and does not necessarily represent the official views of the National Institute of Biomedical Imaging and Bioengineering or the National Institutes of Health. The National Measurement Institute declares that it has no competing interests and by conducting this study does not imply endorsement of the technologies described in the manuscript. C.M.H. and B.J.H. are full-time employees of Bio-Rad Laboratories, Inc. We thank P. Armishaw and D. Burke for their critical review of the manuscript.

REFERENCES

(1) Sykes, P. J.; Neoh, S. H.; Brisco, M. J.; Hughes, E.; Condon, J.; Morley, A. A. *Biotechniques* **1992**, *13*, 444−449.

(2) Vogelstein, B.; Kinzler, K. W. *Proc. Natl. Acad. Sci. U.S.A.* **1999**, *96*, 9236−9241.

(3) Sanders, R.; Huggett, J. F.; Bushell, C. A.; Cowen, S.; Scott, D. J.; Foy, C. A. *Anal. Chem.* **2011**, *83*, 6474−6484.

(4) Lo, Y. M.; Lun, F. M.; Chan, K. C.; Tsui, N. B.; Chong, K. C.; Lau, T. K.; Leung, T. Y.; Zee, B. C.; Cantor, C. R.; Chiu, R. W. *Proc. Natl. Acad. Sci. U.S.A.* **2007**, *104*, 13116−13121.

(5) Wang, J.; Ramakrishnan, R.; Tang, Z.; Fan, W.; Kluge, A.; Dowlati, A.; Jones, R. C.; Ma, P. C. *Clin. Chem.* **2010**, *56*, 623−632.

(6) Dube, S.; Qin, J.; Ramakrishnan, R. *PLoS One* **2008**, *3*, e2876.

(7) Bhat, S.; Herrmann, J.; Armishaw, P.; Corbisier, P.; Emslie, K. R. *Anal. Bioanal. Chem.* **2009**, *394*, 457−467.

(8) Hindson, B. J.; Ness, K. D.; Masquelier, D. A.; Belgrader, P.; Heredia, N. J.; Makarewicz, A. J.; Bright, I. J.; Lucero, M. Y.; Hiddessen, A. L.; Legler, T. C.; Kitano, T. K.; Hodel, M. R.; Petersen, J. F.; Wyatt, P. W.; Steenblock, E. R.; Shah, P. H.; Bousse, L. J.; Troup, C. B.; Mellen, J. C.; Wittmann, D. K.; Erndt, N. G.; Cauley, T. H.; Koehler, R. T.; So, A. P.; Dube, S.; Rose, K. A.; Montesclaros, L.; Wang, S.; Stumbo, D. P.; Hodges, S. P.; Romine, S.; Milanovich, F. P.; White, H. E.; Regan, J. F.; Karlin-Neumann, G. A.; Hindson, C. M.; Saxonov, S.; Colston, B. W. *Anal. Chem.* **2011**, *83*, 8604−8610.

(9) Bhat, S.; Curach, N.; Mostyn, T.; Bains, G. S.; Griffiths, K. R.; Emslie, K. R. *Anal. Chem.* **2010**, *82*, 7185−7192.

(10) Weaver, S.; Dube, S.; Mir, A.; Qin, J.; Sun, G.; Ramakrishnan, R.; Jones, R. C.; Livak, K. J. *Methods* **2010**, *50*, 271−276.

(11) Abramoff, M. D.; Magalhaes, P. J.; Ram, S. J. *Biophoton. Int.* **2004**, *11*, 36−42.

(12) Joint Committee for Guides in Metrology Working Group 2. *International Vocabulary of Metrology - Basic and general concepts and associated terms* (VIM); http://www.bipm.org/utils/common/documents/jcgm/JCGM_200_2008.pdf, 3rd ed.; BIPM: Sèvres Cedex, France, 2008.

(13) Heyries, K. A.; Tropini, C.; Vaninsberghe, M.; Doolin, C.; Petriv, O. I.; Singhal, A.; Leung, K.; Hughesman, C. B.; Hansen, C. L. *Nat. Methods* **2011**, *8*, 649−651.

(14) Pekin, D.; Skhiri, Y.; Baret, J. C.; Le Corre, D.; Mazutis, L.; Salem, C. B.; Millot, F.; El Harrak, A.; Hutchison, J. B.; Larson, J. W.; Link, D. R.; Laurent-Puig, P.; Griffiths, A. D.; Taly, V. *Lab Chip* **2011**, *11*, 2156−2166.

(15) Griffiths, K. R.; Burke, D. G.; Emslie, K. R. *Anal. Methods* **2011**, *3*, 2201−2211.